



Modelling Complex Inlet Geometries in CFD

applied to air flow in ventilated rooms

Skovgaard, M.; Nielsen, Peter V.

Publication date:
1991

Document Version
Publisher's PDF, also known as Version of record

[Link to publication from Aalborg University](#)

Citation for published version (APA):
Skovgaard, M., & Nielsen, P. V. (1991). *Modelling Complex Inlet Geometries in CFD: applied to air flow in ventilated rooms*. Dept. of Building Technology and Structural Engineering. Indoor Environmental Technology Vol. R9149 No. 21

General rights

Copyright and moral rights for the publications made accessible in the public portal are retained by the authors and/or other copyright owners and it is a condition of accessing publications that users recognise and abide by the legal requirements associated with these rights.

- Users may download and print one copy of any publication from the public portal for the purpose of private study or research.
- You may not further distribute the material or use it for any profit-making activity or commercial gain
- You may freely distribute the URL identifying the publication in the public portal -

Take down policy

If you believe that this document breaches copyright please contact us at vbn@aub.aau.dk providing details, and we will remove access to the work immediately and investigate your claim.

INSTITUTTET FOR BYGNINGSTEKNIK
DEPT. OF BUILDING TECHNOLOGY AND STRUCTURAL ENGINEERING
AALBORG UNIVERSITETSCENTER • AUC • AALBORG • DANMARK

INDOOR ENVIRONMENTAL TECHNOLOGY
PAPER NO. 21

**Presented at the 12th AIVC Conference on Air Movement and Ventilation
Control within Buildings, Ottawa, Canada, September 1991**

M. SKOVGAARD & P. V. NIELSEN
MODELLING COMPLEX INLET GEOMETRIES IN CFD - APPLIED TO
AIR FLOW IN VENTILATED ROOMS
DECEMBER 1991

ISSN 0902-7513 R9149

The papers on INDOOR ENVIRONMENTAL TECHNOLOGY are issued for early dissemination of research results from the Indoor Environmental Technology Group at the University of Aalborg. These papers are generally submitted to scientific meetings, conferences or journals and should therefore not be widely distributed. Whenever possible reference should be given to the final publications (proceedings, journals, etc.) and not to the paper in this series.

INDOOR ENVIRONMENTAL TECHNOLOGY
PAPER NO. 21

**Presented at the 12th AIVC Conference on Air Movement and Ventilation
Control within Buildings, Ottawa, Canada, September 1991**

M. SKOVGAARD & P. V. NIELSEN
MODELLING COMPLEX INLET GEOMETRIES IN CFD - APPLIED TO
AIR FLOW IN VENTILATED ROOMS
DECEMBER 1991

ISSN 0902-7513 R9149

MODELLING COMPLEX INLET GEOMETRIES IN CFD - APPLIED TO AIR FLOW IN VENTILATED ROOMS

Skovgaard, M. and Nielsen P.V.
The University of Aalborg, Denmark

SUMMARY

Modern inlet devices applied in the field of ventilation of rooms are getting more complex in terms of geometry in order to fulfil the occupants' demand for thermal comfort in the room and in order to decrease the energy consumption. This expresses the need for a more precise calculation of the flow field. In order to apply CFD for this purpose it is essential to be able to model the inlet conditions precisely and effectively, in a way which is comprehensible to the manufacturer of inlet devices and in a way which can be coped with by the computer.

In this paper a universal method is presented and tested. The method is based upon three-dimensional - and radial wall jet theory and upon diffuser specific experimental data.

Simulations are held up against a more basic method and full-scale measurements. The inlet model is evaluated in terms of result, computational effort and applicability. Promising results are obtained.

LIST OF SYMBOLS

A	Area		
a	Coefficient in difference equation, area		
C_1	Constant in the turbulence model		
C_2	Constant in the turbulence model		
C_D	Constant in the turbulence model		
C_μ	Constant in the turbulence model		
E	Wall roughness function in the logarithmic law		
F	Force		
I	Turbulence intensity		
k	Turbulent kinetic energy		
K	Factor in wall jet formula		
n	Air change rate, normal to surface		
P	Pressure		
PD	Percentage Dissatisfied people due to draught		
Re	Reynolds' number ($\rho l U / \mu$)		
S	Source term		
Tu	Turbulence intensity		
u,v,w	Velocity fluctuations		
U,V,W	Mean velocities		
U^+	Dimensionless velocity parallel to the surface (U_p / U_τ)		
x,y,z	Directions		
y	Normal distance from wall		
y+	Dimensionless wall distance ($U_\tau y_p \rho / \mu$)		
		Subscripts	
		D	Downstream point
		E	East point
		i,j,k	Indicators of direction
		N	North point
		o	Inlet
		P	Centre point
		r	Radial
		rm	Recirculation maximum
		S	Shear, south point
		t	Turbulent
		U	Upstream point
		W	West point
		Greek	
		δ	Kronecker delta, wall jet width, area
		ϵ	Energy dissipation
		θ	Angle
		κ	von Karman constant
		μ	Viscosity (dynamic)
		ρ	Density
		τ	Shear stress
		σ	Constant in the turbulence model (the turbulent Prandtl number)
		ϕ	Generalized variable

INTRODUCTION

Numerical prediction of air flow patterns in mechanically ventilated rooms has been a research object for almost two decades. Up through the 1970's and 1980's Computational Fluid Dynamics (CFD) showed that it was possible to predict the flow field in large domains with relatively small openings (see e.g. *Nielsen 1976*, *Nielsen et al. 1978* or *Gosman et al. 1980*).

In recent years the field of ventilation engineering has started to look upon CFD as a design and an analysing tool, because CFD offers a radical change in available analytical tools, by which the engineer can predict the impact of a certain design of an air condition system on the indoor climate and the energy management of real buildings. But in contrast to most test carried out with CFD, real buildings and air condition systems are often very complex in terms of building - and air supply device geometry (fig. 1), which gives rise to very complex flow phenomena such as transitional flow regimes etc.

The aim of the work reported in the present paper is to look into the influences of a modern complex air supply terminal used in the mixing type of ventilation. The ideas may just as well be applied in the field of displacement ventilation.

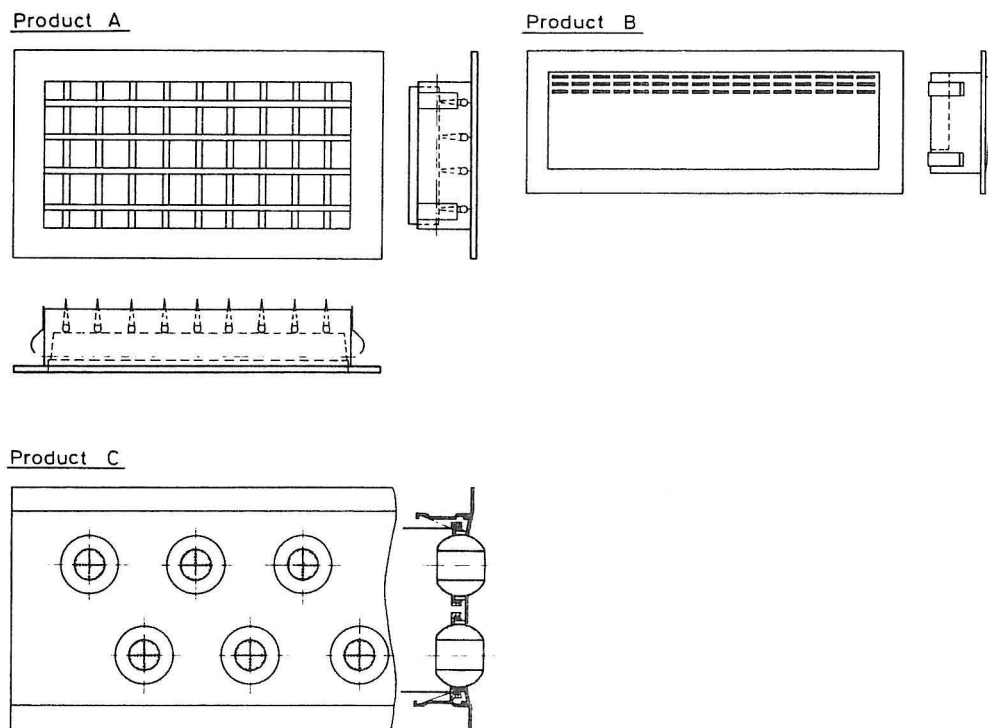


Figure 1. Different designs of air inlet devices.

It is well known that the velocity level in a room ventilated by a mixing type of ventilation is strongly influenced by the supply conditions (*Nielsen 1976*) and that it is

the momentum flow of the inlet which has the major impact of the flow pattern in the room (except maybe for very low inlet velocities). It is also known that the momentum flow in a wall jet created by the jet from the inlet diffuser is lower than the inlet momentum flow (McRee *et al.* 1967). It is therefore very important that the model of the inlet device is able to produce the wall jet momentum either direct by a model of the inlet device or by use of empirical data. In Nielsen 1976 a method is presented which fulfils these basic requirements by use of diffuser specific data. This fact makes also the method quite universal. The model presented in the following utilizes the same basic ideas.

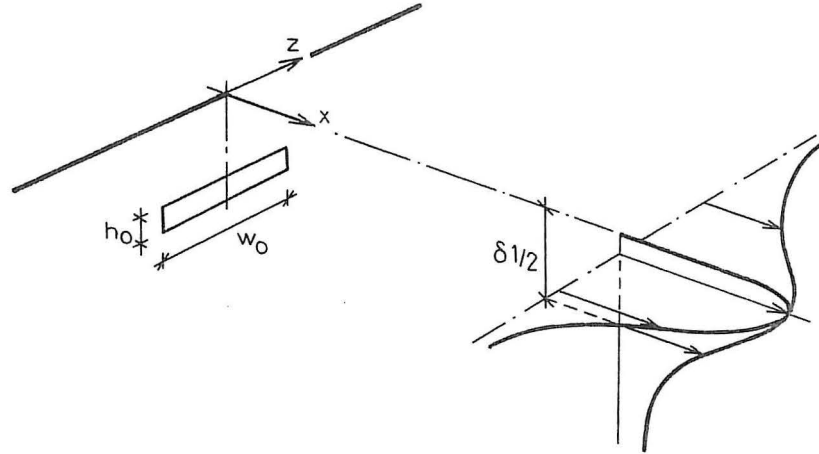


Figure 2. Typical flow from a wall mounted diffuser.

Fig. 2 shows a typical mounting of an inlet device in a wall. The flow from the inlet creates a wall jet type of flow in a certain distance from the inlet, either because the inlet flow is directed upwards or because it is influenced by the Coanda effect. An attempt to model the inlet direct would in most cases require too much computational effort to be realistic. Another more comprehensible way would be to prescribe the actual wall jet conditions in a volume where the flow has adopted this character. Such a method implies that device specific data are available.

MATHEMATICAL MODEL

The mathematical model of the flow is described by the following equations.

The time-averaged continuity or mass conservation equation

$$\frac{\partial}{\partial x_i}(\rho U_i) = 0 \quad (1)$$

The time-averaged momentum equations

$$\frac{\partial}{\partial x_i}(\rho U_i U_j) = - \frac{\partial P}{\partial x_i} + \frac{\partial}{\partial x_i}(-\rho \overline{u_i u_j}) + \frac{\partial}{\partial x_i} \left(\mu \left(\frac{\partial U_i}{\partial x_j} + \frac{\partial U_j}{\partial x_i} \right) \right) \quad (2)$$

where U_i is the time mean velocity of the direction x_i and u_i is the fluctuating velocity in the x_i direction.

To solve the above set of equations it is necessary to represent the fluctuating velocity by a set of turbulence equations. There are several of such models available, but the most suitable model for practical engineering is the k - ϵ model which is a two-equation semi-empirical model for turbulent kinetic energy and its dissipation. The k - ϵ model takes up the eddy viscosity concept by describing the Reynolds stresses in the following way

$$-\rho \overline{u_i u_j} = \mu_t \left(\frac{\partial U_i}{\partial x_j} + \frac{\partial U_j}{\partial x_i} \right) - \frac{2}{3} \rho k \delta_{ij}$$

By substituting the eddy viscosity concept into (2) we obtain the following equation for the mean flow

$$\frac{\partial(\rho U_i U_j)}{\partial x_i} = - \frac{\partial P}{\partial x_i} + \frac{\partial}{\partial x_i} \left((\mu_t + \mu) \left(\frac{\partial U_i}{\partial x_j} + \frac{\partial U_j}{\partial x_i} \right) \right) - 2 \rho k \delta_{ij} \quad (3)$$

$$\text{where } \mu_t = C_\mu \rho \frac{k^2}{\epsilon} \quad (4)$$

The closure equations for k and ϵ will be transport equations of the following form

$$\frac{\partial(\rho U_i k)}{\partial x_i} = \frac{\partial}{\partial x_i} \left(\frac{\mu_t}{\sigma_k} \frac{\partial k}{\partial x_i} \right) + \mu_t \frac{\partial U_i}{\partial x_j} \left(\frac{\partial U_i}{\partial x_j} + \frac{\partial U_j}{\partial x_i} \right) - C_D \rho \epsilon \quad (5)$$

$$\frac{\partial(\rho U_i \epsilon)}{\partial x_i} = \frac{\partial}{\partial x_i} \left(\frac{\mu_t}{\sigma_\epsilon} \frac{\partial \epsilon}{\partial x_i} \right) + C_1 \frac{\epsilon}{k} \mu_t \frac{\partial U_i}{\partial x_j} \left(\frac{\partial U_i}{\partial x_j} + \frac{\partial U_j}{\partial x_i} \right) - \frac{\epsilon}{k} C_2 \rho \epsilon \quad (6)$$

where k and ϵ have the definition

$$k = \frac{1}{2} \overline{u_i u_i}$$

$$\epsilon = \frac{\mu}{\rho} \frac{\partial^2 \overline{u_i u_i}}{\partial x_j^2 \partial x_j}$$

For fully turbulent flow the following set of constants is assigned

$$C_\mu = 0.09; C_1 = 1.44; C_2 = 1.92; \sigma_k = 1.0; \sigma_\epsilon = 1.3; C_D = 1.0$$

NUMERICAL PROCEDURE

The computational domain is divided into a number of cells by a non-uniform, staggered and rectangular mesh in order to produce finer grid close to the walls and in other areas where gradients may be expected to be large. The previous set of equations (3 + 5 + 6) is discretized by the finite volume technique (FV) (*Patankar 1980*) and cast into the following general form:

$$\begin{aligned} a_P \phi_P &= a_E \phi_E + a_W \phi_W + a_N \phi_N + a_S \phi_S + a_D \phi_D + a_U \phi_U + S_\phi \\ S_\phi &= S_C + S_P \phi_P \end{aligned} \quad (7)$$

The pressure is linked via the pressure correction technique and the turbulent viscosity is calculated by (4).

When a surrounding set of boundary conditions is provided a solution can be obtained. Equation (7) is solved by the TMDD technique and an ADI-like procedure.

BOUNDARY CONDITIONS

To be able to solve the discretized set of equations a full set of boundary conditions (BC) must be given because of the elliptic nature of the governing equations. However, the use of the hybrid scheme may have the effect that not all BC's are effective.

Test case

The test room is shown in fig. 3. The inlet device is of the HESCO-type (KS4W205K370) where the flow can be adjusted to any kind of three-dimensional flow. For this purpose all nozzles are adjusted to an angle of 40° upwards.

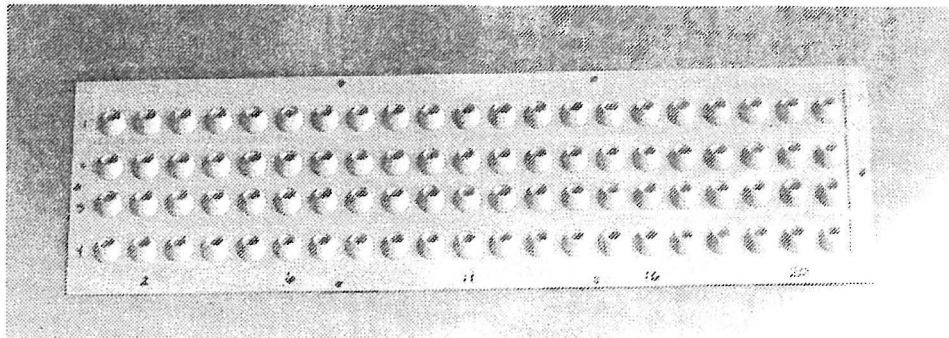
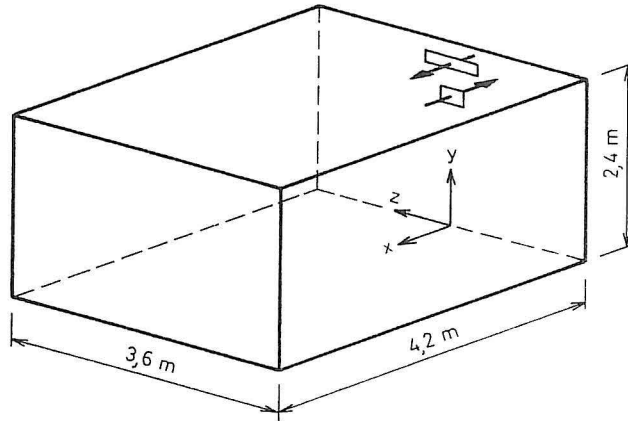


Figure 3. Sketch of the test case. a) The room geometry. b) Close-up of the inlet device.

(i) Boundary conditions at surfaces

Because of the validity range of the set of equations (fully turbulent region) the no-slip boundary conditions have to be introduced indirectly by wall functions in the source term at the first grid node (subscript p). This approach has also the advantage that it spares some grid nodes in the near wall region. However, this method can be difficult to use in areas where the maximum velocity is found close to the surface (e.g. the wall jet region).

The boundary conditions are given by the shear force at the wall (subscript s) and the velocity parallel to the surface in the first gridnode (subscript p)

$$F_s = \delta x_s \tau_s = -\delta x \mu \frac{\partial U}{\partial n}$$

If $y^+ < 11.63$:

$$F_s = -\mu \frac{(U_p - U_s)}{y_p} \delta x \quad (8)$$

If $y^+ > 11.63$:

$$F_s = -\frac{\rho C_D C_\mu^{\frac{1}{4}} k_p^{\frac{1}{2}} (U_p - U_s)}{U^+} \delta x \quad (9)$$

$$U^+ = \frac{1}{\kappa} \ln(E y^+) ; \quad k_p = \frac{U_\tau^2}{\sqrt{C_\mu}} ; \quad \kappa = 0.4187 ; \quad E = 9.793$$

F_s is subtracted as a source term in the near wall cell in the point p with ϕ_p equal to u_p and $u_s = 0$.

The limit 11.63 is probably not valid in three-dimensional boundary layer flow and one can argue that it is already too low in the one-dimensional boundary layer but it is, nevertheless, used in this two layer approach.

Turbulent kinetic energy and dissipation:

$$\frac{\partial k}{\partial n} = 0$$

$$\varepsilon = \frac{C_\mu^{\frac{3}{4}} k^{\frac{2}{3}}}{y_p \kappa}$$

(ii) Boundary conditions in the return opening

Outlet U-velocity is set to fulfil the overall continuity so

$$U_{\text{out,uniform}} = \frac{\int_{x_1}^{x_2} \int_{y_1}^{y_2} U_o(x,y) dA}{A_{\text{out}}}$$

Upwind boundary is assumed in the outflow so exact values are not required.

(iii) Inlet boundary conditions

The inlet boundary is particularly complex because we must give an exact image of the real conditions and real conditions often mean a very complicated design of the inlet device. The complex inlet device used in the present test case is chosen to give a complicated flow pattern around the inlet and therefore it is a realistic test of the CFD method. The present inlet device is difficult to model direct because the many small nozzles are distributed over a fairly large area and are directed upwards in an angle of 40°. It is therefore decided to try two simplified approaches to represent the inlet flow conditions.

The two methods tested in the following are: a basic momentum preserving method and a development - or extension of the method outlined by *Gosman et al. 1980*, and further explained by *Nielsen 1989* and *Skovgaard et al. 1990*. The latter method is developed to be general - and to be more comprehensible to the manufacturer. The ideas behind the method are not only useful in most set-ups of the mixing type but also in many displacement systems.

The basic method:

The assumptions for this method are that the momentum flow in the jet created around the inlet should be presented by a more simple model. The distributed nozzles are simulated by a single opening having the same effective inlet area, the same aspect ratio (h/w) and a flow rate equal to the measured one and therefore the same momentum flow as the actual diffuser. The above-mentioned assumptions give following BC's.

$$a_{\text{inlet}} = 0.18 \cdot 0.062 = 0.011 \text{ m}^2$$

$$a_o = f(U_o)$$

$$\begin{aligned} \text{for } n = 1 &: 0.008 \text{ m}^2 \\ \text{for } n = 3 &: 0.00855 \text{ m}^2 \\ \text{for } n = 6 &: 0.009 \text{ m}^2 \end{aligned}$$

$$U_o = 3.6 \text{ m/s} : U_{\text{inlet}} = 2.71 \text{ m/s}, V_{\text{inlet}} = 2.27, W_{\text{inlet}} = 0.0 \text{ (n = 3)}$$

$$k_{\text{inlet}} = 1.5 \cdot I^2 U_{\text{inlet}}^2, I = 0.1$$

$$\epsilon_{\text{inlet}} = C_{\mu}^{3/4} k^{3/2} / l$$

The "prescribed velocity" PV method:

When the PV method is used the velocity profiles for U and V are prescribed in a full volume in front of the diffuser at a location where the wall jet type of flow is established and therefore has a parabolic nature, see *Nielsen 1989*. This method requires data for the behaviour of the real flow. Tests were carried out on the chosen inlet geometry by *Skovgaard et al. 1990*. The tests showed that the maximum velocity of the wall jet is described by

$$U_r = K(\theta) U_0 \frac{\sqrt{a_0}}{x+x_0} \quad (10)$$

where the K-factor for this particular inlet is interpolated from experimental data (*Skovgaard et al. 1990*) (fig. 4).

$$K(\theta) = 4.2 - 0.975\theta - 8.206\theta^2 + 7.828\theta^3 - 2.088\theta^4 \quad (11)$$

θ is in rad.

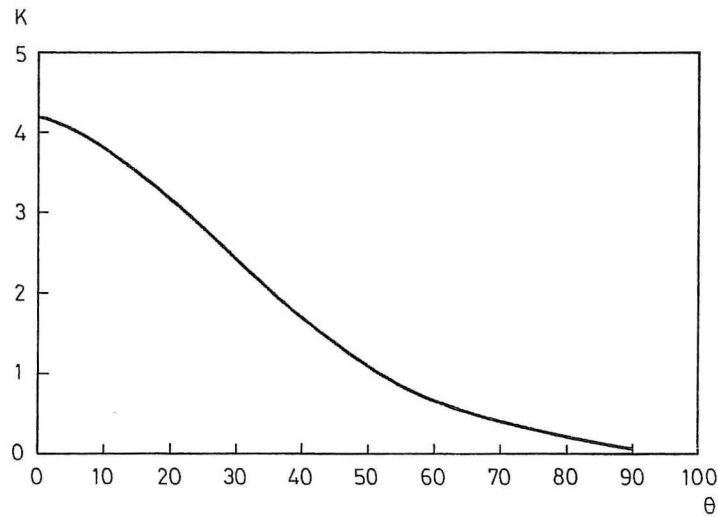


Figure 4. $K(\theta)$ interpolated from eksperimental data.

U and V are calculated from

$$\begin{aligned} U &= \cos\theta U_r \\ V &= \sin\theta U_r \end{aligned}$$

U and V profiles are self-similar up to a distance of $y/\delta_{1/2} = 1.0$ under the ceiling

(Nielsen 1989). The following wall jet profile is assumed (Verhoff 1963)

$$f\left(\frac{y}{\delta_1}\right) = 1.4794 \left(\frac{y}{\delta_1}\right)^{\frac{1}{7}} \left(1 - \operatorname{erf}\left(0.6775 \left(\frac{y}{\delta_1}\right)\right)\right)$$

and δ is taken from Skovgaard *et al.* 1990:

$$\frac{\delta_1(x)}{2} = 0.08(x + 0.45)$$

RESULTS

Simulated results from the basic model and the PV model will in the following be compared with measured data for air change rates 1, 3 and 6 h⁻¹.

The overall flow patterns for the cases are shown in fig. 5 and 6.

Predictions in the basic model show that the radial jet below the ceiling, fig. 5g, has a component of very high velocity directed against the corners. This flow pattern may be the result of the impingement at the ceiling and it has the effect that a high velocity level is obtained in the occupied zone.

The velocity distribution below the ceiling in case of the PV model has a characteristic "peak" along the centre line, fig. 6g. This is in the experiments observed as an area with parallel flow. Measurements by Heikkinen 1991 have also shown this combination of two-/three-dimensional flow and radial flow. The maximum velocity in the occupied zone is close to the measured level which shows the practical relevance of the PV model.

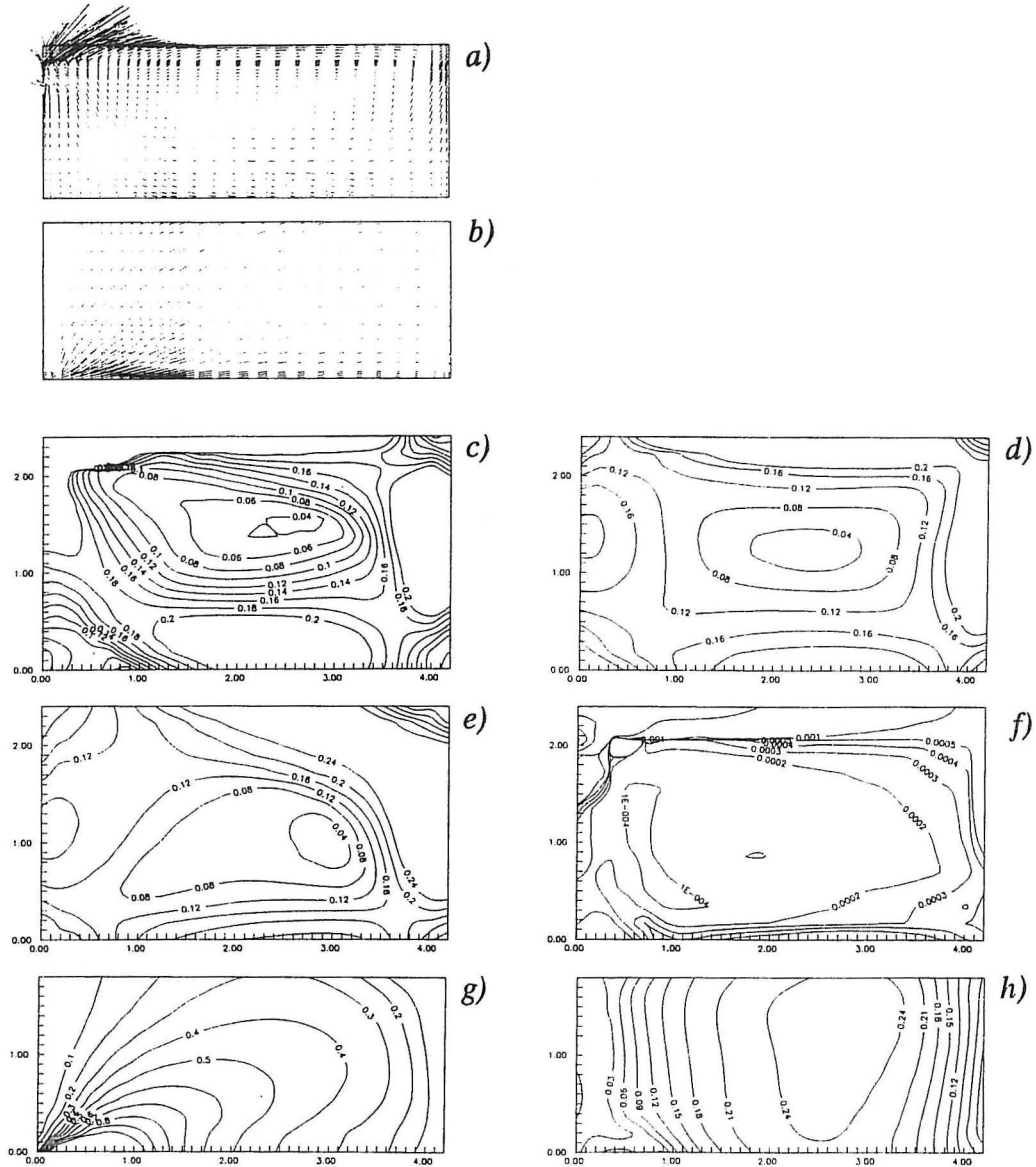
The area with the maximum velocity, U_{m} , in the occupied zone is located very close to the wall opposite the supply opening (Skovgaard *et al.* 1990). The predictions are not able to reproduce this location.

The results in fig.7 relate to the measured data by Skovgaard *et al.* 1990. The figure depicts the decay of the centre line velocity. x_0 is measured to 0.45 m behind the inlet. $a_0^{1/2}$ is a function of the inlet Reynolds number and it is again taken from the measured data.

It is seen that discrepancies are found in both simulations due to the very complex flow structure in the real case. In the basic model case the peak velocity decreases too rapidly caused by the flow going outward towards the corners. If we instead focus on the PV model it is seen that although discrepancies are present the decay is simulated

with higher accuracy.

The predictions indicate that a good description of the boundary conditions is a necessary requirement for the prediction of fully turbulent flow pattern with acceptable accuracy.



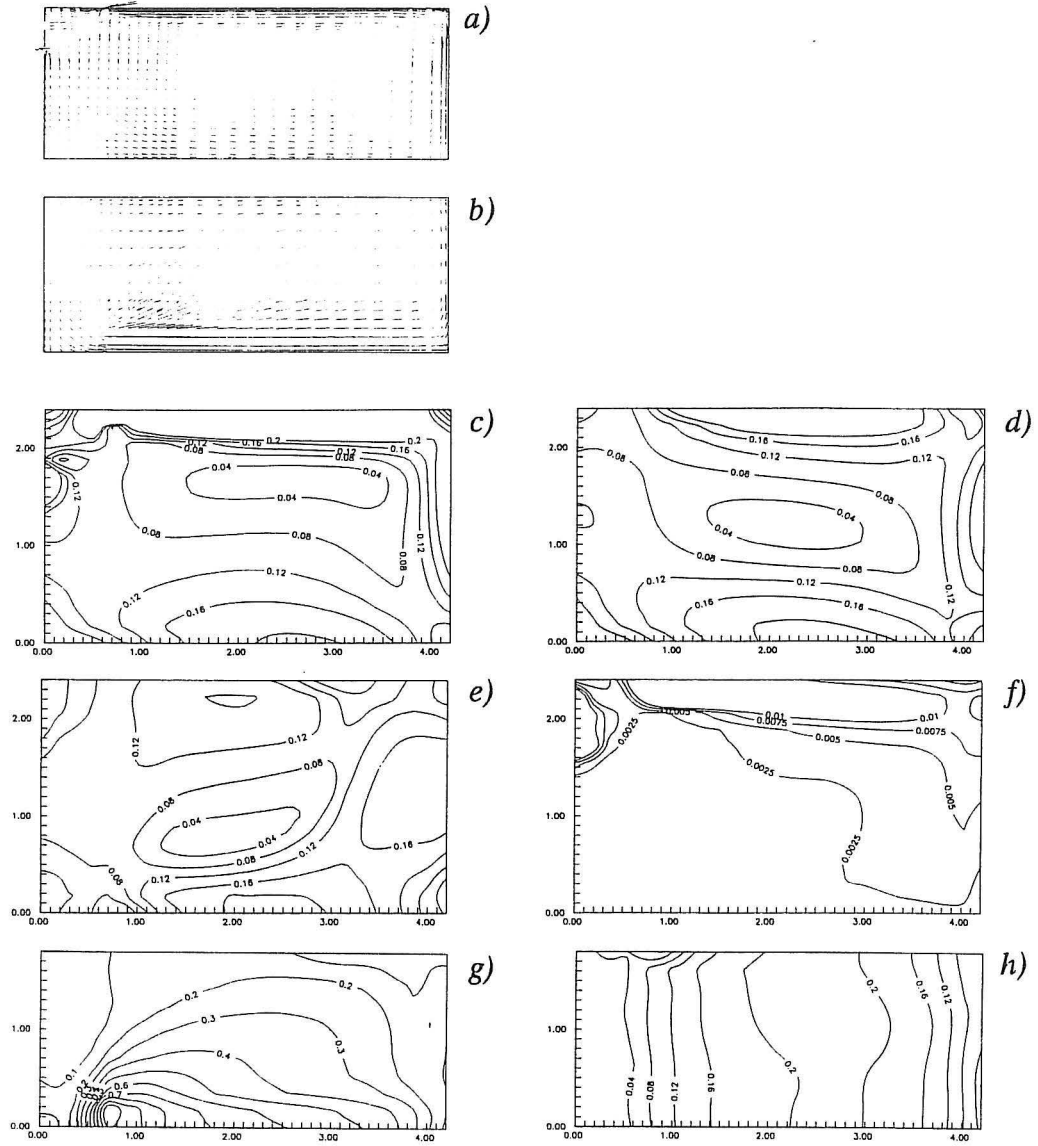


Figure 6. Air flow patterns from the PV model ($n = 3h^{-1}$). a) Velocity vectors in the centre line. b) Velocity vector in a plane 0.04 m below the ceiling. c)-e) Speed contours in the planes $z = 0.02$, 1.0 and 1.7 m. f) Iso-kinetic energy in plane $z = 0.02$. g)-h) Speed contours in $y = 0.05$ and $y = 2.36$.

One of the main purposes of a design method is to predict the maximum velocity in the occupied zone. Fig. 9 shows the measured and the predicted maximum velocity U_{rm} . The figure shows that the PV method for description of the supply opening is giving the best estimate of U_{rm} . But it can also be seen that the performance is poor for $n = 1$ in both models because the low Reynolds number effect has a large impact on the flow at low velocities.

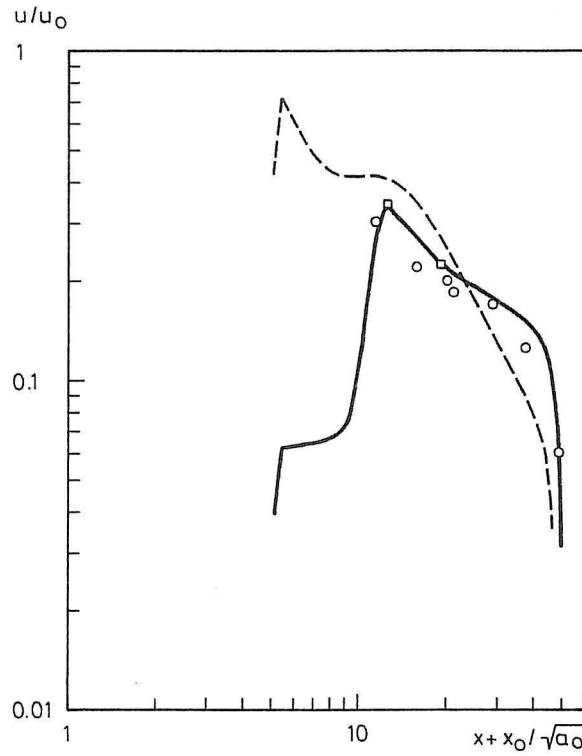


Figure 7. Measured and simulated decay of peak centre-line velocity ($n = 3h^{-1}$). o - measured, dashed line - basic model and line - PV model (the PV volume is indicated by squares).

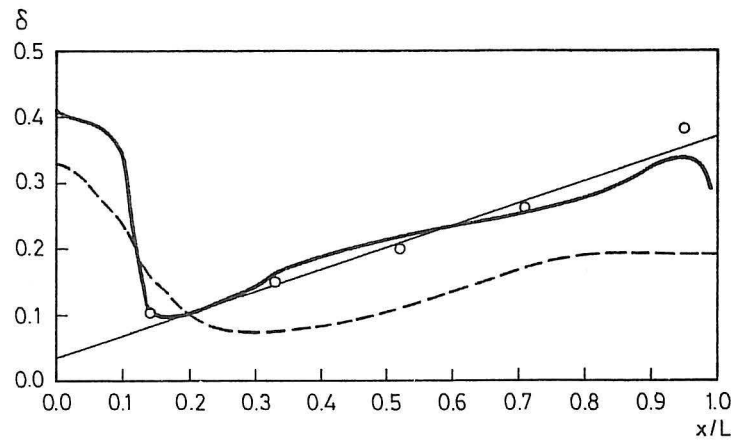


Figure 8. Spread of the wall jet in the centre plane. (o - measured, dashed line - basic model and line - PV model.)

Several authors have made studies of this phenomenon (see e.g. Skovgaard *et al.* 1990, Murakami 1983, Chen 1979 or Restivo 1979) but it has not led to any prediction of it because the k, ϵ model supposes a fully turbulent flow. The low Reynolds number effect in fig. 9 arises partly from the supply device and partly from the flow in the

room, see (Skovgaard *et al.* 1990). The basic model can incorporate the change in the effective area, a_o , and the PV model can in addition to this also include variations in the prescribed volume up to a distance of $x=1.35\text{m}$. The effects are not very obvious in any of the predictions. This is partly because the change in $K(\theta)$ as a function of air change rate has not been taken into account in the PV model (a mean of the measured K factors is used). But it is also because a large part of the low Reynolds' phenomena is occurring inside the flow and therefore cannot be described by the boundary conditions. Further investigations in this specific area have to be done.

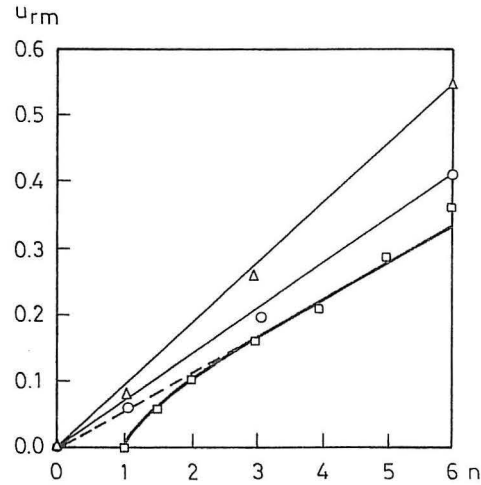


Figure 9. U_{rm} as a function of air change rate. Squares - experiments, triangles - basic model, o - PV model.

As previously mentioned one of the major forces with CFD analysis of flow fields is the very detailed knowledge of the velocity, turbulence and thermal parameters in the room. These data can be used in a comfort analysis of the room or of the occupied zone. In fig. 10 such an application is shown where the PD index (percent dissatisfied) is calculated (Fanger *et al.* 1989).

The calculation is given as an example and the same equation is therefore used for the full room and for the foot level, although it is known that the draught tolerance is slightly higher at foot level. The following comfort equation is used

$$PD = (34 - t_{air})(U - 0.05)^{0.62}(0.37UTu + 3.14)$$

where

$$Tu = \frac{\sqrt{k}}{1.1U}$$

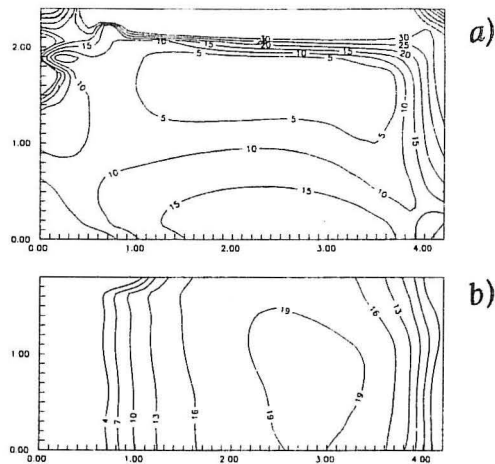


Figure 10. Calculated PD index. a) $z = 0.02$. b) Foot height approx. 5 cm above the floor.

CONCLUSION

CFD simulations of air flow patterns in ventilated spaces give detailed information of comfort parameters and are therefore useful as an analysis and design tool.

A good representation of the boundary conditions is a necessary requirement for prediction of fully turbulent flow. Two inlet models have been tested. One with the aim to model the supply device direct (basic) and one which models the resulting flow pattern in a volume in front of the diffuser (PV). The latter method which requires diffuser specific data has clearly the best performance. The first method fails to meet one basic requirement namely to reproduce the overall flow pattern. The second method gives also the lowest computational cost for the simulated case.

The PV model is still the best choice if low Reynolds' number effects are present because it can incorporate low Reynolds' number effects from the inlet device and from the resulting flow up to the border of the volume in a certain distance from the inlet.

The simulation indicates that low Reynolds' number effects not only arise from the inlet device and the boundary layer but from the flow in the room. This part of the low Reynolds number effects can therefore not be taken into account by solely modifying the boundary conditions.

REFERENCES

Chen, Q., Suter, P. and Moser, A.
Influence of Air diffusion. Energy systems laboratory series. Federal Inst. of Tech, ETH, Zürich Switzerland 1990.

PAPERS ON INDOOR ENVIRONMENTAL TECHNOLOGY

PAPER NO. 1: C. E. Hyldgård: *Aerodynamic Control of Exhaust*. ISSN 0902-7513 R8712.

PAPER NO. 2: Per Heiselberg, Peter V. Nielsen: *The Contaminant Distribution in a Ventilated Room with Different Air Terminal Devices*. ISSN 0902-7513 R8713.

PAPER NO. 3: Peter V. Nielsen, L. Evensen, Peter Grabau, J. H. Thulesen-Dahl: *Air Distribution in Rooms with Ceiling-Mounted Obstacles and Three-Dimensional Flow*. ISSN 0902-7513 R8714.

PAPER NO. 4: Peter V. Nielsen, Åke T. A. Möller: *Measurements on Buoyant Wall Jet Flows in Air-Conditioned Rooms*. ISSN 0902-7513 R8715.

PAPER NO. 5: Peter V. Nielsen: *Numerical Prediction of Air Distribution in Rooms. Status and Potentials*. ISSN 0902-7513 R8823.

PAPER NO. 6: Peter V. Nielsen, Åke T. Möller: *Measurements on Buoyant Jet Flows from a Ceiling-Mounted Slot Diffuser*. ISSN 0902-7513 R8832.

PAPER NO. 7: Peter Kofoed, Peter V. Nielsen: *Thermal Plumes in Ventilated Rooms - An Experimental Research Work*. ISSN 0902-7513 R8833.

PAPER NO. 8: Peter V. Nielsen, Lars Hoff, Lars Germann Pedersen: *Displacement Ventilation by Different Types of Diffusers*. ISSN 0902-7513 R8834.

PAPER NO. 9: Per Heiselberg, Peter V. Nielsen: *Flow Conditions in a Mechanically Ventilated Room with a Convective Heat Source*. ISSN 0902-7513 R8835.

PAPER NO. 10: Peter V. Nielsen: *Displacement Ventilation in a Room with Low-Level Diffusers*. ISSN 0902-7513 R8836.

PAPER NO. 11: Peter V. Nielsen: *Airflow Simulation Techniques - Progress and Trends*. ISSN 0902-7513 R8926.

PAPER NO. 12: M. Skovgaard, C. E. Hyldgaard & P. V. Nielsen: *High and Low Reynolds Number Measurements in a Room with an Impinging Isothermal Jet*. ISSN 0902-7513 R9003

PAPER NO. 13: M. Skovgaard, P. V. Nielsen: *Numerical Prediction of Air Distribution in Rooms with Ventilation of the Mixing Type using the Standard K, ϵ -Model*. ISSN 0902-7513 R9042.

PAPER NO. 14: P. Kofoed, P. V. Nielsen: *Thermal Plumes in Ventilated Rooms - Measurements in Stratified Surroundings and Analysis by Use of an Extrapolation Method*. ISSN 0902-7513 R9043.

PAPER NO. 15: P. Heiselberg, M. Sandberg: *Convection from a Slender Cylinder in a Ventilated Room*. ISSN 0902-7513 R9044.

PAPERS ON INDOOR ENVIRONMENTAL TECHNOLOGY

PAPER NO. 16: C. E. Hyldgaard: *Water Evaporation in Swimming Baths*. ISSN 0902-7513 R9045.

PAPER NO. 17: H. Overby, M. Steen-Thøde: *Calculation of Vertical Temperature Gradients in Heated Rooms*. ISSN 0902-7513 R9046.

PAPER NO. 18: P. V. Nielsen, U. Madsen, D. Tveit: *Experiments on an Exhaust Hood for the Paint Industry*. ISSN 0902-7513 R9146.

PAPER NO. 19: L. Germann Pedersen, P. V. Nielsen: *Exhaust System Reinforced by Jet Flow*. ISSN 0902-7513 R9147.

PAPER NO. 20: P. V. Nielsen: *Models for the Prediction of Room Air Distribution*. ISSN 0902-7513 R9148.

PAPER NO. 21: M. Skovgaard, P. V. Nielsen: *Modelling Complex Inlet Geometries in CFD - Applied to Air Flow in Ventilated Rooms*. ISSN 0902-7513 R9149.

PAPER NO. 22: M. Skovgaard, P. V. Nielsen: *Numerical Investigation of Transitional Flow over a Backward Facing Step using a Low Reynolds Number $k - \epsilon$ Model*. ISSN 0902-7513 R9150.

PAPER NO. 23: P. Kofoed, P. V. Nielsen: *Auftriebsströmungen verschiedener Wärmequellen - Einfluss der umgebenden Wände auf den geförderten Volumenstrom*. ISSN 0902-7513 R9151.

PAPER NO. 24: P. Heiselberg: *Concentration Distribution in a Ventilated Room under Isothermal Conditions*. ISSN 0902-9152.

Department of Building Technology and Structural Engineering
The University of Aalborg, Sohngaardsholmsvej 57. DK 9000 Aalborg
Telephone: 45 98 15 85 22 Telefax: 45 98 14 82 43